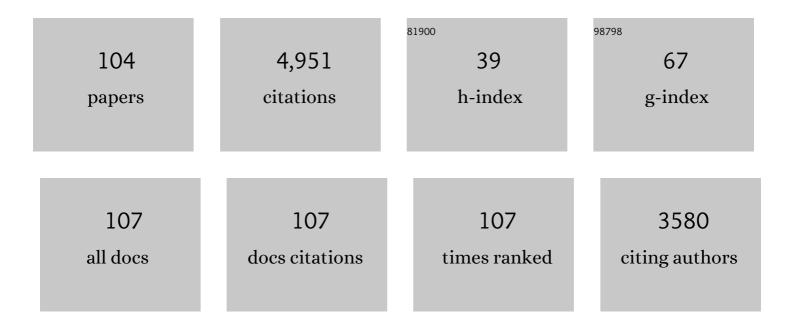
## Ching-Long Lin

List of Publications by Year in descending order

Source: https://exaly.com/author-pdf/8692354/publications.pdf Version: 2024-02-01



#	Article	IF	CITATIONS
1	A stable discretization of the lattice Boltzmann equation for simulation of incompressible two-phase flows at high density ratio. Journal of Computational Physics, 2005, 206, 16-47.	3.8	555
2	Characteristics of the turbulent laryngeal jet and its effect on airflow in the human intra-thoracic airways. Respiratory Physiology and Neurobiology, 2007, 157, 295-309.	1.6	268
3	Mass preserving nonrigid registration of CT lung images using cubic Bâ€spline. Medical Physics, 2009, 36, 4213-4222.	3.0	185
4	Large-eddy simulation of turbulent flow in a channel with rib roughness. International Journal of Heat and Fluid Flow, 2003, 24, 372-388.	2.4	161
5	Regional Deposition of Particles in an Image-Based Airway Model: Large-Eddy Simulation and Left-Right Lung Ventilation Asymmetry. Aerosol Science and Technology, 2011, 45, 11-25.	3.1	141
6	A Characteristic Galerkin Method for Discrete Boltzmann Equation. Journal of Computational Physics, 2001, 171, 336-356.	3.8	136
7	Simulation of pulmonary air flow with a subject-specific boundary condition. Journal of Biomechanics, 2010, 43, 2159-2163.	2.1	131
8	Supine and prone differences in regional lung density and pleural pressure gradients in the human lung with constant shape. Journal of Applied Physiology, 2009, 107, 912-920.	2.5	130
9	On intra- and intersubject variabilities of airflow in the human lungs. Physics of Fluids, 2009, 21, 101901.	4.0	128
10	An Eulerian description of the streaming process in the lattice Boltzmann equation. Journal of Computational Physics, 2003, 185, 445-471.	3.8	113
11	Numerical simulation of unsteady multidimensional free surface motions by level set method. International Journal for Numerical Methods in Fluids, 2003, 42, 853-884.	1.6	111
12	Association of Dysanapsis With Chronic Obstructive Pulmonary Disease Among Older Adults. JAMA - Journal of the American Medical Association, 2020, 323, 2268.	7.4	104
13	The effects of geometry on airflow in the acinar region of the human lung. Journal of Biomechanics, 2009, 42, 1635-1642.	2.1	94
14	Rarefaction and compressibility effects of the lattice-Boltzmann-equation method in a gas microchannel. Physical Review E, 2005, 71, 046706.	2.1	90
15	A multiscale MDCT image-based breathing lung model with time-varying regional ventilation. Journal of Computational Physics, 2013, 244, 168-192.	3.8	85
16	Computational fluid dynamics. IEEE Engineering in Medicine and Biology Magazine, 2009, 28, 25-33.	0.8	81
17	Human airway branch variation and chronic obstructive pulmonary disease. Proceedings of the National Academy of Sciences of the United States of America, 2018, 115, E974-E981.	7.1	80
18	Quantitative computed tomographic imaging–based clustering differentiates asthmatic subgroups with distinctive clinical phenotypes. Journal of Allergy and Clinical Immunology, 2017, 140, 690-700.e8.	2.9	79

#	Article	IF	CITATIONS
19	A level set characteristic Galerkin finite element method for free surface flows. International Journal for Numerical Methods in Fluids, 2005, 49, 521-547.	1.6	78
20	Registration-based assessment of regional lung function via volumetric CT images of normal subjects vs. severe asthmatics. Journal of Applied Physiology, 2013, 115, 730-742.	2.5	77
21	Airway Wall Stiffening Increases Peak Wall Shear Stress: A Fluid–Structure Interaction Study in Rigid and Compliant Airways. Annals of Biomedical Engineering, 2010, 38, 1836-1853.	2.5	73
22	The comprehensive imaging-based analysis of the lung. Academic Radiology, 2004, 11, 1370-1380.	2.5	67
23	Quantitative assessment of multiscale structural and functional alterations in asthmatic populations. Journal of Applied Physiology, 2015, 118, 1286-1298.	2.5	67
24	Multiscale imageâ€based modeling and simulation of gas flow and particle transport in the human lungs. Wiley Interdisciplinary Reviews: Systems Biology and Medicine, 2013, 5, 643-655.	6.6	66
25	Numerical Study of High-Frequency Oscillatory Air Flow and Convective Mixing in a CT-Based Human Airway Model. Annals of Biomedical Engineering, 2010, 38, 3550-3571.	2.5	64
26	Lattice Boltzmann method on composite grids. Physical Review E, 2000, 62, 2219-2225.	2.1	61
27	Effect of Carrier Gas Properties on Aerosol Distribution in a CT-based Human Airway Numerical Model. Annals of Biomedical Engineering, 2012, 40, 1495-1507.	2.5	54
28	Pressure evolution lattice-Boltzmann-equation method for two-phase flow with phase change. Physical Review E, 2003, 67, 056703.	2.1	53
29	Large-Eddy Simulation of Turbulent Flow over a Fixed Two-Dimensional Dune. Journal of Hydraulic Engineering, 2006, 132, 643-651.	1.5	49
30	A cubic B-spline-based hybrid registration of lung CT images for a dynamic airway geometric model with large deformation. Physics in Medicine and Biology, 2011, 56, 203-218.	3.0	49
31	A Numerical Study of Heat and Water Vapor Transfer in MDCT-Based Human Airway Models. Annals of Biomedical Engineering, 2014, 42, 2117-2131.	2.5	49
32	Assessment of regional ventilation and deformation using 4D-CT imaging for healthy human lungs during tidal breathing. Journal of Applied Physiology, 2015, 119, 1064-1074.	2.5	48
33	Prediction of Darcy–Forchheimer drag for micro-porous structures of complex geometry using the lattice Boltzmann method. Journal of Micromechanics and Microengineering, 2006, 16, 2240-2250.	2.6	47
34	Large eddy simulation of turbulent open-channel flow with free surface simulated by level set method. Physics of Fluids, 2005, 17, 025108.	4.0	46
35	The effect of surface roughness on flow structures in a neutrally stratified planetary boundary layer flow. Physics of Fluids, 1997, 9, 3235-3249.	4.0	45
36	Estimation of thermal and mass diffusivity in a porous medium of complex structure using a lattice Boltzmann method. International Journal of Heat and Mass Transfer, 2008, 51, 3913-3923.	4.8	45

#	Article	IF	CITATIONS
37	The lung physiome: merging imagingâ€based measures with predictive computational models. Wiley Interdisciplinary Reviews: Systems Biology and Medicine, 2009, 1, 61-72.	6.6	45
38	Characteristics of airflow in a CT-based ovine lung: a numerical study. Journal of Applied Physiology, 2007, 102, 1469-1482.	2.5	44
39	A lattice Boltzmann algorithm for calculation of the laminar jet diffusion flame. Journal of Computational Physics, 2006, 215, 133-152.	3.8	43
40	An unstructured finite volume approach for structural dynamics in response to fluid motions. Computers and Structures, 2008, 86, 684-701.	4.4	42
41	Imageâ€based modeling of lung structure and function. Journal of Magnetic Resonance Imaging, 2010, 32, 1421-1431.	3.4	39
42	Improved CT-based estimate of pulmonary gas trapping accounting for scanner and lung-volume variations in a multicenter asthmatic study. Journal of Applied Physiology, 2014, 117, 593-603.	2.5	37
43	Multiscale imaging and registration-driven model for pulmonary acinar mechanics in the mouse. Journal of Applied Physiology, 2013, 114, 971-978.	2.5	35
44	Assessment of regional non-linear tissue deformation and air volume change of human lungs via image registration. Journal of Biomechanics, 2014, 47, 1626-1633.	2.1	35
45	Coherent Structures In Open-Channel Flows Over a Fixed Dune. Journal of Fluids Engineering, Transactions of the ASME, 2005, 127, 858-864.	1.5	33
46	Steady streaming: A key mixing mechanism in low-Reynolds-number acinar flows. Physics of Fluids, 2011, 23, 41902.	4.0	33
47	Retrieval of Microscale Flow Structures from High-Resolution Doppler Lidar Data Using an Adjoint Model. Journals of the Atmospheric Sciences, 2004, 61, 1500-1520.	1.7	30
48	A 4DCT imaging-based breathing lung model with relative hysteresis. Journal of Computational Physics, 2016, 326, 76-90.	3.8	30
49	Differentiation of quantitative CT imaging phenotypes in asthma versus COPD. BMJ Open Respiratory Research, 2017, 4, e000252.	3.0	30
50	Effect of static vs. dynamic imaging on particle transport in CT-based numerical models of human central airways. Journal of Aerosol Science, 2016, 100, 129-139.	3.8	29
51	Automatic construction of subject-specific human airway geometry including trifurcations based on a CT-segmented airway skeleton and surface. Biomechanics and Modeling in Mechanobiology, 2017, 16, 583-596.	2.8	28
52	Evaluation of Lobar Biomechanics during Respiration Using Image Registration. Lecture Notes in Computer Science, 2009, 12, 739-746.	1.3	28
53	A Simple Finite-Volume Formulation of the Lattice Boltzmann Method for Laminar and Turbulent Flows. Numerical Heat Transfer, Part B: Fundamentals, 2010, 58, 242-261.	0.9	25
54	Imaging-based clusters in former smokers of the COPD cohort associate with clinical characteristics: the SubPopulations and intermediate outcome measures in COPD study (SPIROMICS). Respiratory Research, 2019, 20, 153.	3.6	25

#	Article	IF	CITATIONS
55	1D network simulations for evaluating regional flow and pressure distributions in healthy and asthmatic human lungs. Journal of Applied Physiology, 2019, 127, 122-133.	2.5	25
56	Lattice Boltzmann Study of Bubble Dynamics. Numerical Heat Transfer, Part B: Fundamentals, 2006, 50, 333-351.	0.9	24
57	Retrieval of Urban Boundary Layer Structures from Doppler Lidar Data. Part I: Accuracy Assessment. Journals of the Atmospheric Sciences, 2008, 65, 3-20.	1.7	24
58	Early Airway Structural Changes in Cystic Fibrosis Pigs as a Determinant of Particle Distribution and Deposition. Annals of Biomedical Engineering, 2014, 42, 915-927.	2.5	23
59	A four-dimensional computed tomography comparison of healthy and asthmatic human lungs. Journal of Biomechanics, 2017, 56, 102-110.	2.1	23
60	Airway Gas Flow. , 2011, 1, 1135-1157.		22
61	Numerical simulations of aerosol delivery to the human lung with an idealized laryngeal model, image-based airway model, and automatic meshing algorithm. Computers and Fluids, 2017, 148, 1-9.	2.5	22
62	Local tissue-weight-based nonrigid registration of lung images with application to regional ventilation. Proceedings of SPIE, 2009, , .	0.8	21
63	Efficient methods for implementation of multi-level nonrigid mass-preserving image registration on GPUs and multi-threaded CPUs. Computer Methods and Programs in Biomedicine, 2016, 127, 290-300.	4.7	21
64	A Feasible Computational Fluid Dynamics Study for Relationships of Structural and Functional Alterations with Particle Depositions in Severe Asthmatic Lungs. Computational and Mathematical Methods in Medicine, 2018, 2018, 1-12.	1.3	21
65	Differences in Particle Deposition Between Members of Imaging-Based Asthma Clusters. Journal of Aerosol Medicine and Pulmonary Drug Delivery, 2019, 32, 213-223.	1.4	21
66	Large Eddy Simulation of Internal Boundary Layers Created by a Change in Surface Roughness. Journals of the Atmospheric Sciences, 2002, 59, 1697-1711.	1.7	20
67	Large Eddy Simulation of an Inhomogeneous Atmospheric Boundary Layer under Neutral Conditions. Journals of the Atmospheric Sciences, 2002, 59, 2479-2497.	1.7	20
68	Imaging-based clusters in current smokers of the COPD cohort associate with clinical characteristics: the SubPopulations and Intermediate Outcome Measures in COPD Study (SPIROMICS). Respiratory Research, 2018, 19, 178.	3.6	20
69	Near-grid-scale energy transfer and coherent structures in the convective planetary boundary layer. Physics of Fluids, 1999, 11, 3482-3494.	4.0	19
70	Transport and deposition of hygroscopic particles in asthmatic subjects with and without airway narrowing. Journal of Aerosol Science, 2020, 146, 105581.	3.8	18
71	Retrieval of Flow Structures in a Convective Boundary Layer Using an Adjoint Model: Identical Twin Experiments. Journals of the Atmospheric Sciences, 2001, 58, 1767-1783.	1.7	17
72	A CPU-based symmetric non-rigid image registration method in human lung. Medical and Biological Engineering and Computing, 2018, 56, 355-371.	2.8	17

#	Article	IF	CITATIONS
73	Local pressure-transport structure in a convective atmospheric boundary layer. Physics of Fluids, 2000, 12, 1112-1128.	4.0	15
74	Retrieval of Urban Boundary Layer Structures from Doppler Lidar Data. Part II: Proper Orthogonal Decomposition. Journals of the Atmospheric Sciences, 2008, 65, 21-42.	1.7	15
75	A Numerical Study of Water Loss Rate Distributions in MDCT-Based Human Airway Models. Annals of Biomedical Engineering, 2015, 43, 2708-2721.	2.5	15
76	Lung Lobar Slippage Assessed with the Aid of Image Registration. Lecture Notes in Computer Science, 2010, 13, 578-585.	1.3	15
77	Large-eddy simulation of air flow around a wall-mounted circular cylinder and a tripod tower. Journal of Turbulence, 2007, 8, N29.	1.4	13
78	Lumen area change (Delta Lumen) between inspiratory and expiratory multidetector computed tomography as a measure of severe outcomes in asthmatic patients. Journal of Allergy and Clinical Immunology, 2018, 142, 1773-1780.e9.	2.9	13
79	Structural and Functional Features on Quantitative Chest Computed Tomography in the Korean Asian versus the White American Healthy Non-Smokers. Korean Journal of Radiology, 2019, 20, 1236.	3.4	13
80	An integrated mathematical epithelial cell model for airway surface liquid regulation by mechanical forces. Journal of Theoretical Biology, 2018, 438, 34-45.	1.7	12
81	Latent traits of lung tissue patterns in former smokers derived by dual channel deep learning in computed tomography images. Scientific Reports, 2021, 11, 4916.	3.3	12
82	An integrated 1D breathing lung simulation with relative hysteresis of airway structure and regional pressure for healthy and asthmatic human lungs. Journal of Applied Physiology, 2020, 129, 732-747.	2.5	10
83	Quantitative computed tomography determined regional lung mechanics in normal nonsmokers, normal smokers and metastatic sarcoma subjects. PLoS ONE, 2017, 12, e0179812.	2.5	10
84	CFD Simulation of Contaminant Decay for High Reynolds Flow in a Controlled Environment. Annals of Occupational Hygiene, 2010, 54, 88-99.	1.9	9
85	A numerical study of gas transport in human lung models. , 2005, , .		8
86	Contributions of Kinetic Energy and Viscous Dissipation to Airway Resistance in Pulmonary Inspiratory and Expiratory Airflows in Successive Symmetric Airway Models With Various Bifurcation Angles. Journal of Biomechanical Engineering, 2018, 140, .	1.3	8
87	Longitudinal Imaging-Based Clusters in Former Smokers of the COPD Cohort Associate with Clinical Characteristics: The SubPopulations and Intermediate Outcome Measures in COPD Study (SPIROMICS). International Journal of COPD, 2021, Volume 16, 1477-1496.	2.3	8
88	CT-derived 3D-diaphragm motion in emphysema and IPF compared to normal subjects. Scientific Reports, 2021, 11, 14923.	3.3	8
89	On the Smoothness Constraints for Four-Dimensional Data Assimilation. Journal of Computational Physics, 2002, 181, 430-453.	3.8	7
90	Quantitative CT-based structural alterations of segmental airways in cement dust-exposed subjects. Respiratory Research, 2020, 21, 133.	3.6	7

6

#	Article	IF	CITATIONS
91	Assessment and validation of a hygroscopic growth model with different water activity estimation methods. Aerosol Science and Technology, 2020, 54, 1169-1182.	3.1	7
92	Aerosol deposition predictions in computed tomography-derived skeletons from severe asthmatics: A feasibility study. Clinical Biomechanics, 2019, 66, 81-87.	1.2	6
93	Generation-based study of airway remodeling in smokers with normal-looking CT with normalization to control inter-subject variability. European Journal of Radiology, 2021, 138, 109657.	2.6	6
94	Estimation of Turbulent Viscosity and Diffusivity in Adjoint Recovery of Atmospheric Boundary Layer Flow Structures. Multiscale Modeling and Simulation, 2003, 1, 196-220.	1.6	5
95	Application of a Nonhydrostatic Model to Flow in a Free Surface Fish Passage Facility. Journal of Hydraulic Engineering, 2008, 134, 993-999.	1.5	4
96	A Perfect Match Condition for Point-Set Matching Problems Using the Optimal Mass Transport Approach. SIAM Journal on Imaging Sciences, 2013, 6, 730-764.	2.2	4
97	Use of Large-Eddy Simulation to Characterize Roughness Effect of Turbulent Flow Over a Wavy Wall. Journal of Fluids Engineering, Transactions of the ASME, 2003, 125, 1075-1077.	1.5	4
98	Large Eddy Simulation of Wind Flow over A Realistic Urban Area. Computation, 2020, 8, 47.	2.0	3
99	In silico methods to model dose deposition. , 2021, , 167-195.		3
100	Cluster-Guided Multiscale Lung Modeling via Machine Learning. , 2018, , 1-20.		2
101	Machine learning and in silico methods. , 2021, , 375-390.		2
102	Detection of smoothly distributed spatial outliers, with applications to identifying the distribution of parenchymal hyperinflation following an airway challenge in asthmatics. Statistics in Medicine, 2017, 36, 1638-1654.	1.6	1
103	Coherent Structures in Open-Channel Flows Over a Fixed Dune. , 2004, , 575.		0

104 Cluster-Guided Multiscale Lung Modeling via Machine Learning. , 2020, , 2699-2718.

0